

ARTICLE

Model-based assessment of neutrophil-mediated phagocytosis and digestion of bacteria across in vitro and in vivo studies

Anders Thorsted  | Anh Duc Pham  | Lena E. Friberg  | Elisabet I. Nielsen 

Department of Pharmacy, Uppsala University, Uppsala, Sweden

Correspondence

Elisabet I. Nielsen, Department of Pharmacy, Box 580, Uppsala 751 23, Sweden.
Email: elisabet.nielsen@farmaci.uu.se

Present address

Anh Duc Pham, Leiden Academic Centre for Drug Research, Leiden University, Leiden, The Netherlands

Abstract

Neutrophil granulocytes are key components of the host response against pathogens, and severe neutropenia, with neutrophil counts below 0.5×10^6 cells/mL, renders patients increasingly vulnerable to infections. Published in vitro ($n=7$) and in vivo ($n=5$) studies with time-course information on bacterial and neutrophil counts were digitized to characterize the kinetics of neutrophil-mediated bacterial killing and inform on the immune systems' contribution to the clearance of bacterial infections. A mathematical model for the in vitro dynamics of bacteria and the kinetics of neutrophil-mediated phagocytosis and digestion was developed, which was extended to in vivo studies in immune-competent and immune-compromised mice. Neutrophil-mediated bacterial killing was described by two first-order processes—phagocytosis and digestion—scaled by neutrophil concentration, where 50% of the maximum was achieved at neutrophil counts of 1.19×10^6 cells/mL (phagocytosis) and 6.55×10^6 cells/mL (digestion). The process efficiencies diminished as the phagocytosed bacteria to total neutrophils ratio increased (with 50% reduction at a ratio of 3.41). Neutrophil in vivo dynamics were captured through the characterization of myelosuppressive drug effects and postinoculation neutrophil influx into lungs and by system differences (27% bacterial growth and 9.3% maximum capacity, compared with in vitro estimates). Predictions showed how the therapeutically induced reduction of neutrophil counts enabled bacterial growth, especially when falling below 0.5×10^6 cells/mL, whereas control individuals could deal with all tested bacterial burdens (up to 10^9 colony forming units/g lung). The model-based characterization of neutrophil-mediated bacterial killing simultaneously predicted data across in vitro and in vivo studies and may be used to inform the capacity of host-response at the individual level.

Anders Thorsted and Anh Duc Pham contributed equally to this work.

This is an open access article under the terms of the [Creative Commons Attribution-NonCommercial](https://creativecommons.org/licenses/by-nc/4.0/) License, which permits use, distribution and reproduction in any medium, provided the original work is properly cited and is not used for commercial purposes.

© 2023 The Authors. *CPT: Pharmacometrics & Systems Pharmacology* published by Wiley Periodicals LLC on behalf of American Society for Clinical Pharmacology and Therapeutics.

Study Highlights

WHAT IS THE CURRENT KNOWLEDGE ON THE TOPIC?

Neutrophils are important contributors to the host's innate immune response against pathogens, but low counts render the host vulnerable to infections.

WHAT QUESTION DID THIS STUDY ADDRESS?

This study integrates in vitro and in vivo data in a modeling framework to study neutrophil-mediated bacterial killing and the relationships between neutrophil and bacterial counts in terms of clearance or manifestation of an infection.

WHAT DOES THIS STUDY ADD TO OUR KNOWLEDGE?

This study provides quantitative insights into the neutrophil–bacterial axis, and may serve as a translational link between in vitro and in vivo studies.

HOW MIGHT THIS CHANGE DRUG DISCOVERY, DEVELOPMENT, AND/OR THERAPEUTICS?

The results improve the understanding of preclinical data for antibiotic drug development, specifically the contribution of the innate immune response in studies with immune-competent mice.

INTRODUCTION

Neutrophils play a key role in the host innate immune response against invading pathogens.^{1,2} Granulopoiesis by hematopoietic bone marrow cells generate up toward 2×10^{11} neutrophils per day, which circulate with a half-life of 6–8 h.³ The normal blood neutrophil range in humans is defined as $1.5\text{--}8.0 \times 10^6$ cells/mL. Neutropenia, a blood neutrophil count below 1.5×10^6 cells/mL, is associated with an increased infection risk and more severe infections.^{4,5} Among typical pathogens found in neutropenic patients, often with respiratory or blood stream infections, are the gram-negatives *Escherichia coli*, *Klebsiella* species, *Pseudomonas aeruginosa*, and *Acinetobacter baumannii* and the gram-positives *Staphylococcus epidermidis* and *Staphylococcus aureus*.^{6,7}

Infection occurs when an invading pathogen takes residence in the sterile tissues of a host and starts to proliferate. Pathogen associated molecular patterns are recognized immediately by the host innate immune system, which engages to liberate the body of the invader. Pathogens are marked with opsonin molecules to facilitate phagocytosis, either by the complement arm of the innate immune system (by opsonin molecules C4b, C3b, and C3bi) or by immunoglobulin G antibodies, which enable phagocyte recognition by way of complement or Fc receptors.^{4,8–10} Eradication proceeds through the internalization of the pathogen (phagocytosis) and the breakdown of the internalized matter (“digestion”). Phagocytosis triggers at the cell membrane through stimulation of initiating receptors, which leads to intracellular activation and formation of pseudopodia (arm-like extensions) and an

engulfed phagosome, after which intracellular granules containing reactive oxygen species and enzymes digest the phagosome.^{8,11}

Neutropenia is often a complication in cancer patients who receive myelosuppressive chemotherapy, as dividing hematopoietic cells are affected in addition to the targeted cancerous cells.¹² The Common Terminology Criteria for Adverse Events defines increasingly severe neutropenia (Grades 2 to 4) as ≥ 1.0 to $<1.5 \times 10^6$ cells/mL, ≥ 0.5 to $<1.0 \times 10^6$ cells/mL, and $<0.5 \times 10^6$ cells/mL. To avoid prolonged neutropenia and the increased risk of opportunistic infections and sepsis, neutrophils should recover prior to a next chemotherapeutic dose administration, with treatment decisions possibly guided by predictive models.^{13,14}

Typically, antimicrobial drugs are administered to assist a compromised (or functioning) immune system in combating an infection. However, the host response component is usually disregarded during pharmacokinetic/pharmacodynamic (PKPD) assessment of antibiotics, and its effect relative to that of the administered antibiotic(s) is undetermined, although it may be profound.^{15,16} Although large variability may exist between individuals, all sustain a degree of phagocytic capacity, which warrants further investigation of the relation between bacterial concentration and neutrophil-mediated killing capacity. Application of mechanism-based mathematical PKPD modeling has been shown to offer substantial value for optimized antimicrobial therapy by allowing description of the full time courses of drug disposition, bacterial growth, antibiotic killing, and resistance development.¹⁷ In a model-based analysis, data from different sources (e.g., in vitro, in vivo, clinical)

can be combined to establish a translational framework, which furthers understanding and quantification of differences and similarities between settings.¹⁷ To expand these models, and to also integrate a quantitative assessment of the interaction between pathogen and the host immune system, has recently been highlighted as a prioritized research area and a step toward successful prediction of individual patient outcomes and clinical trial results.¹⁸

The aim of this work was to use mathematical modeling to characterize the kinetics of neutrophil-mediated phagocytosis and digestion of bacteria to quantify the ability of the immune system to eradicate different degrees of bacterial burdens. Specifically, neutrophil-mediated killing was characterized across varying neutrophil and bacterial concentrations (in vitro studies) and extended to describe neutrophil and bacterial time courses in immune-competent and compromised mice (in vivo studies).

MATERIALS AND METHODS

A literature search was performed to identify studies describing temporal dynamics of neutrophils and bacteria. Studies that used pathogenic bacteria and reported bacterial (colony forming units [CFU]) or neutrophil concentration over time were included. Studies performed in vitro should use $\geq 5\%$ human serum (for opsonization) and a temperature of 37°C, whereas in vivo studies should be performed using a murine pneumonia model. The identified studies, listed in Table 1, comprised seven in vitro and five in vivo studies with information relevant for the intended modeling work.

The in vitro experiments, either performed in liquid or gel media, were done at one fixed neutrophil concentration but with varying bacterial inoculum^{19–22} or by varying both the bacterial inoculum and the neutrophil concentration.^{16,23,24} Bacterial concentrations (CFU/mL) were quantified by bacterial plating, followed by incubation and counting of CFUs. Two studies specifically assessed neutrophil digestion, by first exposing bacteria to neutrophils before removal of extracellular bacteria.^{20,22} The quantified CFU then represented viable intracellular bacteria (i.e., phagocytosed but nondigested bacteria), with the difference reflecting digestion of phagocytosed bacteria. In one study, the viable extracellular bacteria were separated from neutrophils by centrifugation, with the quantified CFU representing viable nonphagocytosed bacteria.¹⁹ The remaining studies lysed the neutrophils with sterilized water to release intracellular bacteria, and the quantified CFU represented the total viable CFU (i.e., nonphagocytosed and phagocytosed but nondigested).^{16,21,23,24} One study was reserved for evaluation and not used for model building.¹⁶

The in vivo experiments consisted of four studies of *A. baumannii* pneumonia^{25–28} and one study that quantified neutrophil concentrations in tissues (without bacteria).²⁹ In one study, mice were pretreated with cyclophosphamide (50/50, 100/50, 200/150 mg/kg, or vehicle 96 and 24 h prior to inoculation) to reduce the circulating neutrophil count, which was assumed to impact the post-inoculation neutrophil influx and thus CFU time course in lung.²⁷ Three studies described the bacterial time course in lung of immune-competent mice,^{25,26,28} and one also informed on the time course of neutrophils and alveolar macrophages in lung.²⁸ At specified times after inoculation, mice were euthanized and the lungs were carefully dissected and homogenized prior to plating. The units of the digitized observations were transformed from CFU/lung or CFU/mL to CFU/g by considering the dilution volume and/or an approximate lung weight of 0.175 g in C57BL/6 mice.³⁰ The reported bacterial inoculum was also transformed (from CFU to CFU/g).

Software

Graphical data points representing longitudinal bacteria or neutrophil were digitized by use of Engauge digitizer (Version 12.1). The statistical software R (Version 4.0.2) was used for data visualization and model predictions using packages tidyverse (Version 1.3.1)³¹ and RxODE (Version 1.1.2).³² Model development was conducted with NONMEM (Version 7.5.0) using the first-order conditional estimation method facilitated by Perl-speaks-NONMEM and Xpose 4 (Version 4.7.1).³³ The computations were enabled by the Swedish National Infrastructure for Computing (SNIC) at UPPMAX, by resources in the project SNIC 2021/5-552.

Model development

Data were converted to log₁₀ scale and modeled with additive residual error using the transform-both-sides approach. As a starting point, separate models were developed for relevant subsets of the in vitro data in the following order: (i) bacterial growth (without neutrophils), (ii) neutrophil digestion of phagocytosed bacteria,^{20,22} and (iii) neutrophil phagocytosis of bacteria. In each step, the parameters relating to the previous model(s) were fixed with a simultaneous estimation of the combined in vitro model as a final step.

To describe the in vivo data, the established in vitro model was extended to a model for neutrophil dynamics after cancer chemotherapy.^{13,34} Development proceeded in steps to account for (i) drug-induced change in circulating

TABLE 1 Overview of included in vitro and in vivo studies, including the bacterial species, type of bacterial measurement (in vitro), mouse strain (in vivo), bacterial start inoculum, static neutrophil concentration (in vitro) or site of measurement (in vivo), study setup and duration, and reference.

| Study | Bacteria | Bacteria measurement | Inoculum (CFU/mL) | Neutrophil levels (cells/mL) | Study setup (duration) | Reference |
|------------|---|----------------------|--|---|---|-----------|
| In vitro-1 | <i>Staphylococcus epidermidis</i> | Total | 10 ³ , 10 ⁵ , 10 ⁷ | 0; 1, 4, 8 × 10 ⁵ ; 1, 2, 4 × 10 ⁶ | In vitro suspension (0–1.5 h) | 23 |
| In vitro-2 | <i>S. epidermidis</i> | Total | 10 ³ , 10 ⁵ , 10 ⁶ , 10 ⁷ , 10 ⁸ | 0; 2, 4 × 10 ⁵ ; 1, 2, 4 × 10 ⁶ ; 1 × 10 ⁷ | In vitro fibrin gel (0–1.5 h) | 24 |
| In vitro-3 | <i>Staphylococcus aureus</i> , <i>Escherichia coli</i> | Extracellular | 10 ⁶ , 10 ⁷ , 10 ⁸ , 10 ⁹ , 10 ¹⁰ | 0; 5 × 10 ⁶ | In vitro suspension (0–2 h) | 20 |
| In vitro-4 | <i>S. aureus</i> , <i>E. coli</i> | Intracellular | 10 ⁵ , 10 ⁶ , 10 ⁷ , 10 ⁸ | 5 × 10 ⁶ | In vitro suspension (0–2 h) | 19 |
| In vitro-5 | <i>S. aureus</i> | Total | 10 ⁶ , 10 ⁷ , 10 ⁸ | 5 × 10 ⁶ | In vitro suspension (0–2 h) | 21 |
| In vitro-6 | <i>S. aureus</i> , <i>Streptococcus pyogenes</i> , <i>Corynebacterium</i> | Intracellular | 10 ⁵ | 1 × 10 ⁶ | In vitro suspension (0–3 h) | 22 |
| In vitro-7 | <i>S. aureus</i> | Total | 10 ⁴ , 10 ⁶ , 10 ⁷ | 0; 2.5, 5, 7.5 × 10 ⁵ ; 1, 4.4 × 10 ⁶ | In vitro suspension (0–1 h) | 16 |
| Study | Bacteria | Mouse (weeks) | Inoculum (CFU/g) | Neutrophils (site) | Study setup & data range | Reference |
| Mice-1 | <i>Acinetobacter baumannii</i> | C57BL/6 (7–9) | 5.71 × 10 ⁶ , 5.71 × 10 ⁷ | – | In vivo pneumonia (0–72 h) | 25 |
| Mice-2 | <i>A. baumannii</i> | Swiss-Webster (–) | 1.57 × 10 ⁷ | Blood | In vivo pneumonia (0–24 h, cyclophosphamide pretreated) | 27 |
| Mice-3 | <i>A. baumannii</i> | C57BL/6 (8–12) | 5.71 × 10 ⁶ , 5.71 × 10 ⁷ , 5.71 × 10 ⁸ | – | In vivo pneumonia (0–96 h) | 26 |
| Mice-4 | <i>A. baumannii</i> | C57BL/6 (8–12) | ~1.71 × 10 ⁸ | Lung | In vivo pneumonia (0–168 h) | 28 |
| Mice-5 | – | C57BL/6 (6–12) | – | Blood, lung | Tissue neutrophils (steady state) | 29 |

Abbreviation: CFU, colony forming unit.

neutrophils, (ii) neutrophil (and macrophage) time course in lungs upon bacterial deposition, and (iii) CFU time course in lung after bacterial deposition. Structural and numerical (parameter estimates) differences between in vitro and in vivo studies were assessed before a final simultaneous fit with in vitro and in vivo parameters unfixed.

Bacterial in vitro dynamics

A published structural model was adopted to describe bacterial dynamics, separating bacteria into growing (S) and resting (R) states.³⁵ In this model, total CFU count is governed by first-order rate constants describing growth (k_{growth}) and natural death (k_{death}) and by a maximum carrying density (B_{max}), with transfer from S to R defined as $k_{\text{SR}} = (S + R) \cdot (k_{\text{growth}} - k_{\text{death}}) / B_{\text{max}}$.

Bacterial growth controls displayed a growth delay, and a lag state (L) was added.^{19,23,24} Because of the limited data and short duration of experiments (≤ 3 h), the first-order natural bacterial death rate constant was fixed to 0.179 h^{-1} , and k_{RS} was fixed to 0 h^{-1} (determined based on more informative data in the original publication of the model).³⁵ B_{max} was fixed to $2.5 \cdot 10^9 \text{ CFU/mL}$, representing the highest digitized CFU. All bacteria started in the L state and transitioned to the S state (by first-order rate constant k_{lag}) while being subjected to natural death (k_{death}). The bacterial system was defined by:

$$\frac{dL}{dt} = -k_{\text{death}} \cdot L - k_{\text{lag}} \cdot L \quad (1)$$

$$\frac{dS}{dt} = -k_{\text{death}} \cdot S + k_{\text{lag}} \cdot L - k_{\text{SR}} \cdot S + k_{\text{growth}} \cdot S \quad (2)$$

$$\frac{dR}{dt} = -k_{\text{death}} \cdot R + k_{\text{SR}} \cdot S \quad (3)$$

Neutrophil in vitro phagocytosis and digestion

Neutrophils were assumed to eliminate bacteria according to two first-order processes, with estimated rate constants for phagocytosis ($k_{\text{N,phag}}$ from all three states: L, S, and R) and subsequent intracellular digestion ($k_{\text{N,dig}}$).¹¹ Both processes were assumed to have a maximum capacity ($k_{\text{N,max,phag}}$, $k_{\text{N,max,dig}}$) related to the neutrophil concentration (N) through linear, maximum effect [E_{max}], or sigmoidal E_{max} models (with estimated potency parameters $N_{50,\text{phag}}$ and $N_{50,\text{dig}}$).²⁷ As each neutrophil has the capacity for a finite number of bacteria, links were tested between decreasing phagocytosis and digestion rates with an increase in the ratio of phagocytosed bacteria to

total neutrophils (P/N, with 50% reduction at estimated ratios $P/N_{50,\text{phag}}$ and $P/N_{50,\text{dig}}$).³⁶ Time-related decreases in phagocytosis and digestion were assessed ($k_{\text{N,loss,phag}}$, $k_{\text{N,loss,dig}}$), potentially related to decreased opsonisation, overall system fatigue, and a loss of cells.^{20,37} Parameterizations for neutrophil phagocytosis and digestion are given in Equations (4) and (5), whereas the number of bacteria in the neutrophil-phagocytosed state (P_{N}) is captured by Equation (6):

$$k_{\text{N,phag}} = \left(\frac{k_{\text{N,max,phag}} \cdot N}{N_{50,\text{phag}} + N} \right) \cdot \left(1 - \frac{P/N}{P/N_{50,\text{phag}} + P/N} \right) \cdot e^{(-k_{\text{N,loss,phag}} \cdot t)} \quad (4)$$

$$k_{\text{N,dig}} = \left(\frac{k_{\text{N,max,dig}} \cdot N}{N_{50,\text{dig}} + N} \right) \cdot \left(1 - \frac{P/N}{P/N_{50,\text{dig}} + P/N} \right) \cdot e^{(-k_{\text{N,loss,dig}} \cdot t)} \quad (5)$$

$$\frac{dP_{\text{N}}}{dt} = k_{\text{N,phag}} \cdot (L + R + S) - k_{\text{N,dig}} \cdot P_{\text{N}} \quad (6)$$

Neutrophil in vivo dynamics

The cyclophosphamide-driven reduction in circulating neutrophils was described by a semimechanistic model for myelosuppressive drug effects in rats.³⁴ No structural changes were made to the model, but parameters were scaled to mice through allometric scaling by weight using weights of 0.025 kg (mice) and 0.295 kg (rats) and exponents of 0.75, 1.0, and -0.25 for cyclophosphamide clearance (CL), volume of distribution (V), and first-order absorption-rate constant (k_{abs}), respectively.^{27,34,38}

The parameter describing neutrophil maturation time (MTT; with $k_{\text{tr}} = 4/\text{MTT}$) was scaled (exponent of 0.25) and the systemic feedback factor (γ) was fixed to 0.149 (rat estimate, unitless), whereas the drug-effect slope (D_{SLP}) and circulating neutrophil concentration at baseline ($N_{\text{circ},T0}$) were estimated from the data.³⁴ Cyclophosphamide concentration in plasma (CP_{pl}/V) was predicted by mono-exponential absorption (from the absorption compartment, CP_{abs} , following intraperitoneal injection) and elimination ($k_{\text{el}} = \text{CL}/V$) in Equations (7) and (8), with neutrophil dynamics described by Equations (9)–(13):

$$\frac{dCP_{\text{abs}}}{dt} = -k_{\text{abs}} \cdot CP_{\text{abs}} \quad (7)$$

$$\frac{dCP_{\text{pl}}}{dt} = k_{\text{abs}} \cdot CP_{\text{abs}} - k_{\text{el}} \cdot CP_{\text{pl}} \quad (8)$$

$$\frac{dN_{\text{prol}}}{dt} = -k_{\text{tr}} \cdot N_{\text{prol}} + k_{\text{tr}} \cdot N_{\text{prol}} \cdot (1 - D_{\text{SLP}} \cdot CP_{\text{pl}}/V) \cdot (N_{\text{circ},T0}/N_{\text{circ}})^{\gamma} \quad (9)$$

$$\frac{dN_{tr1}}{dt} = -k_{tr} \cdot N_{tr1} + k_{tr} \cdot N_{prol} \quad (10)$$

$$\frac{dN_{tr2}}{dt} = -k_{tr} \cdot N_{tr2} + k_{tr} \cdot N_{tr1} \quad (11)$$

$$\frac{dN_{tr3}}{dt} = -k_{tr} \cdot N_{tr3} + k_{tr} \cdot N_{tr2} \quad (12)$$

$$\frac{dN_{circ}}{dt} = -k_{tr} \cdot N_{circ} + k_{tr} \cdot N_{tr3} \quad (13)$$

Although Equations (9)–(13) were all initialized to $N_{circ,T0}$, the neutrophil baselines in tissues are different, as neutrophil infiltration rate is tissue dependent.²⁹ Additionally, neutrophils will migrate to the infected tissue, increasing the local neutrophil concentration.³⁹ These dynamics were incorporated by extending the previous model with a compartment representing lung neutrophils and by implementing a surge defined by amplitude (N_{AMP}), width (N_{SW}), and center (N_{T0}) in the rate constant describing influx of neutrophils into lungs upon infection, described by:

$$\begin{aligned} \frac{dN_{lung}}{dt} = & -k_{tr} \cdot N_{lung} + k_{tr} \\ & \cdot \left(1 + N_{AMP} / \left(\left((T - N_{T0}) / N_{SW} \right)^6 + 1 \right) \right) \cdot N_{circ} \end{aligned} \quad (14)$$

Similar dynamics were explored for lung alveolar macrophages.²⁸

Neutrophil in vivo phagocytosis

The processes of phagocytosis and digestion in vivo were assumed to be similar to the in vitro setup, although disregarding the lag in bacterial growth (i.e., bacteria starting directly in S) and loss of activity (i.e., $k_{N,loss}=0$). Parameter differences between in vitro and in vivo systems were explored by assessing the statistical improvement in fit, starting with k_{growth} and $k_{N,max}$, and the presence of an additional in vivo phagocytic capability (e.g., lung alveolar macrophages) was evaluated (parametrized as in Equations 4–6).

Model evaluation

Nested models were compared through a likelihood ratio test of their objective function values (OFV), representing a statistical measure of fit, with a $\Delta OFV = -3.84$ considered

statistically significant ($\alpha=0.05$) for one additional parameter. Additional assessments were (i) goodness-of-fit plots (comparing model predictions with observations and evaluating residuals over time), (ii) parameter uncertainty, and (iii) simulation-based visual predictive checks (VPCs).^{16,40}

Model predictions

The established model was used to predict bacterial and neutrophil dynamics in 1000 individuals for three cyclophosphamide regimens (10 mg/kg every week [q1w], 20 mg/kg every 10 days [q10d], and 60 mg/kg every third week [q3w])⁴¹ by using a published population pharmacokinetic model for cancer patients (assuming a body weight of 70 kg).⁴² Interindividual variability (as percent coefficient of variation) was included in $N_{circ,T0}$ (20%) and MTT (15%), in CL (27%) and V (56%), and in the myelo-suppressive drug effect (15%). Bacterial infections were simulated where a bacterial burden of 10^6 to 10^9 CFU/g lung was added on Day 35, that is, at a time when neutrophils were predicted to approach the nadir.

RESULTS

The digitized data (Table 1) included 115 in vitro experiments (403 CFU observations) and 21 in vivo experiments (56 CFU, 5 blood and 16 lung neutrophil observations). The final model structure is presented in Figure 1, and parameter estimates and uncertainties are presented in Table 2. The final NONMEM model code and data file are available as Data S2 and Table S1. The digitized data and VPCs are shown in Figure 2, and external evaluation is shown in Figure 3.

Bacterial growth

Application of the bacterial model described by Equations (1)–(3) characterized bacterial dynamics with a k_{lag} of 0.290 h^{-1} ($t_{1/2}$ of 2.39 h) and a k_{growth} of 1.84 h^{-1} (in vitro doubling time of 0.377 h). Without the lag phase a worse fit ($\Delta OFV = +14.4$) was observed and k_{growth} reduced to 0.751 h^{-1} .

Neutrophil in vitro phagocytosis and digestion

Digestion was described as a first-order process ($k_{N,dig}$) with a maximum ($k_{N,max,dig}$) of 5.61 h^{-1} ($t_{1/2}$ of 0.124 h),

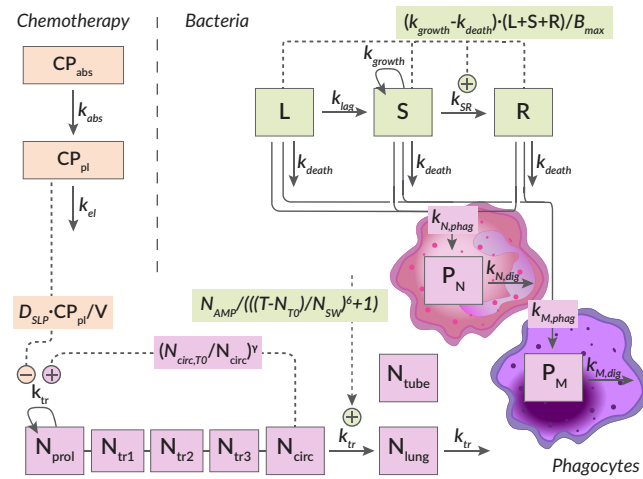


FIGURE 1 Schematic of final model structure connecting the static (N_{tube}) or dynamic (N_{lung}) neutrophil concentration–time course to change in the concentration of bacteria. Bacteria exists in lag (L), growing (S), or resting (R) states and die naturally from all states according to the first-order rate constant k_{death} . Bacteria in L transitions into S (k_{lag}) where they replicate (k_{growth}), and may transition further into R (k_{SR}), dependent on the total number of bacteria ($L + S + R$) in the system in relation to the system carrying density (B_{max}). Bacteria may be phagocytosed in vitro by neutrophils ($k_{N,phag}$) and in vivo by neutrophils ($k_{M,phag}$) and an additional phagocytic capacity ($k_{M,phag}$, represented by a macrophage). Phagocytosis may occur from all three states (L, S, R) after which the bacteria, existing in a phagocytosed state (P_N or P_M), undergo digestion (by $k_{N,dig}$ or $k_{M,dig}$). Deposition of bacteria in the lungs invokes a surge (described by amplitude [N_{AMP}], time [N_{T0}], and width [N_{SW}]) in the rate at which circulating neutrophils (N_{circ}) migrate to the lungs (N_{lung}). The intraperitoneally injected cyclophosphamide (CP_{abs}) is absorbed into plasma (k_{abs}) and eliminated from the system (k_{el}). The cyclophosphamide plasma concentration (CP_{pl}/V) is linked (D_{SLP}) to kill neutrophil progenitors (N_{prol}), which will (delayed by k_{tr} through the neutrophil maturation transit chain N_{tr1} – N_{tr3}) impact the circulating (and by extension lung) neutrophil count.

$N_{50,dig}$ of 3.98×10^6 cells/mL ($\Delta OFV = -25.3$, compared to a linear relation). Improvement was seen when accumulation of bacteria reduced $k_{N,dig}$, with $P/N_{50,dig}$ estimated to 2.84 ($\Delta OFV = -27.9$). Lastly, an exponential time-driven decrease in $k_{N,dig}$ further improved the fit ($\Delta OFV = -23.7$), with a $k_{N,loss,dig}$ of 0.961 h^{-1} ($t_{1/2}$ of 0.721 h). Phagocytosis ($k_{N,phag}$) was described similarly: $k_{N,max,phag}$ of 8.35 h^{-1} ($t_{1/2}$ of 0.0830 h), $N_{50,phag}$ of 6.92×10^5 cells/mL ($\Delta OFV = -133$), $P/N_{50,phag}$ of 3.92 ($\Delta OFV = -151$), and a $k_{N,loss,phag}$ of 0.771 h^{-1} ($t_{1/2}$ of 0.899 h) ($\Delta OFV = -81.9$).

Simplifications were evaluated by allowing shared parameters for digestion and phagocytosis (e.g., one $k_{N,max}$ for both processes). Six parameters could be reduced to three (shared $k_{N,max}$ [$\Delta OFV = +0.033$], $k_{N,loss}$ [$\Delta OFV = +0.837$], and P/N_{50} [$\Delta OFV = +0.95$], with total

$\Delta OFV = +2.12$), whereas separate $N_{50,dig}$ and $N_{50,phag}$ were kept ($\Delta OFV = +6.15$).

Neutrophil in vivo dynamics and bacterial killing

Neutrophil data were adequately described by the chosen structural model, when the slope for cyclophosphamide-induced killing of proliferating cells (D_{SLP} of 1.26 mL/mg) and neutrophil baseline $N_{circ,T0}$ (1.69×10^6 cells/mL) were estimated from the data. The rate of neutrophil influx into the lung peaked approximately 2 days after infection (N_{T0} of 50.5 h) with a large increase (N_{AMP} of 44.2) and with a wide peak duration (N_{SW} of 28.2 h). Reduced bacterial growth and maximum neutrophil activity (k_{growth} of 0.502 h^{-1} and $k_{N,max}$ of 0.820 h^{-1} , $\Delta OFV = -188$), and an additional phagocytic capacity was found in vivo ($k_{M,kill}$ of 0.287 h^{-1} , $\Delta OFV = -23.5$). Although no links could be established between $k_{M,kill}$ and the alveolar macrophage time course, a cyclophosphamide-related reduction in $k_{M,kill}$ (proportional to $N_{circ}/N_{circ,T0}$, $\Delta OFV = -16.9$) and a time-driven reduction ($k_{M,loss}$ of 0.0111 h^{-1} , $\Delta OFV = -5.51$) were identified.

Model predictions

The predicted neutrophil time course in blood and lungs of patients receiving cyclophosphamide according to three different regimens are shown in Figure 4. The predictions illustrate how increased doses of cyclophosphamide impacts circulating and lung influx of neutrophils (reduced peak with CFU inoculation at 5 weeks). The predicted bacterial time course is shown in Figure 5, indicating that untreated individuals are predicted to be able to eradicate the bacteria completely across burdens, although the time of eradication is delayed at higher burdens. More than 50% of patients treated with 10 mg/kg q1w and 20 mg/kg q10d regimens are predicted to handle lower bacterial burdens (10^6 and 10^7 CFU/g lung), but the typical patient fails to eradicate burdens $\geq 10^8$ CFU/g lung, whereas patients treated with a supratherapeutic dose of 60 mg/kg q3w dose fails to combat bacteria at any burden.

DISCUSSION

This work describes the development of a mathematical model (Figure 1) that is able to predict neutrophil-mediated killing of bacteria across in vitro and in vivo experiments through two separate processes that represent phagocytosis and digestion. The model builds on a

TABLE 2 Overview of parameter estimates and uncertainties for each submodel; the combined in vitro growth, phagocytosis, and digestion model; and the final model with simultaneous estimation of in vitro and in vivo models on the entire data set.

| Parameter (units) | | Parameter description | Individual models | | Combined in vitro | | Final model | |
|--|--------------------|---|------------------------|----------|------------------------|---------|------------------------|----------|
| | | | Estimate | (RSE%) | Estimate | (RSE%) | Estimate | (RSE%) |
| Bacterial dynamics—in vitro | | | | | | | | |
| k _{growth} | (h ⁻¹) | Bacterial first-order growth rate constant | 1.90 | (9.9) | 1.56 | (19) | 1.84 | (15) |
| k _{death} | (h ⁻¹) | Bacterial first-order natural death rate constant | 0.179 | (Fixed) | 0.179 | (Fixed) | 0.179 | (Fixed) |
| k _{Iag} | (h ⁻¹) | Bacterial first-order growth-lag rate constant | 0.343 | (32) | 0.420 | (43) | 0.290 | (40) |
| B _{max} | (CFU/mL) | Maximum system capacity | 2.5 × 10 ⁹ | (Fixed) | 2.5 × 10 ⁹ | (Fixed) | 2.5 × 10 ⁹ | (Fixed) |
| ERR ^a ω | (CFU/mL) | Additive error term for in vitro CFU | 0.115 | (10) | 0.279 | (16) | 0.279 | (8.0) |
| Neutrophil-mediated bacterial killing—in vitro | | | | | | | | |
| k _{N,max,dig} | (h ⁻¹) | Neutrophil first-order maximum digestion rate constant | 5.61 | (47) | 8.85 ^b | (14) | 8.85 ^b | (13) |
| k _{N,max,phag} | (h ⁻¹) | Neutrophil first-order maximum phagocytosis rate constant | 8.35 | (11) | | | | |
| k _{N,loss,dig} | (h ⁻¹) | Time-related decrease in neutrophil digestion | 0.961 | (14) | 0.781 ^b | (13) | 0.779 ^b | (13) |
| k _{N,loss,phag} | (h ⁻¹) | Time-related decrease in neutrophil phagocytosis | 0.771 | (11) | | | | |
| N _{50,dig} | (N/mL) | Neutrophil concentration resulting in 50% of maximum digestion rate | 3.98 × 10 ⁶ | (6.2) | 6.46 × 10 ⁶ | (1.5) | 6.55 × 10 ⁶ | (1.4) |
| N _{50,phag} | (N/mL) | Neutrophil concentration resulting in 50% of maximum phagocytosis rate | 6.92 × 10 ⁵ | (5.3) | 1.46 × 10 ⁶ | (4.6) | 1.19 × 10 ⁶ | (4.3) |
| P/N _{50,dig} | (CFU/N) | Phagocytosed bacteria to total neutrophil count reducing digestion rate by 50% | 2.84 | (29) | 3.32 ^b | (21) | 3.41 ^b | (22) |
| P/N _{50,phag} | (CFU/N) | Phagocytosed bacteria to total neutrophil count reducing phagocytosis rate by 50% | 3.92 | (26) | | | | |
| Neutrophil and cyclophosphamide PKPD—in vivo | | | | | | | | |
| CL | (mL/h) | Cyclophosphamide clearance | 0.311 | (Scaled) | – | – | 0.311 | (Scaled) |
| V | (mL) | Cyclophosphamide distribution volume | 0.153 | (Scaled) | – | – | 0.153 | (Scaled) |
| k _a | (h ⁻¹) | Cyclophosphamide first-order absorption rate constant | 20.9 | (Scaled) | – | – | 20.9 | (Scaled) |
| MTT | (h) | Mean transit time for neutrophil bone-marrow maturation | 37.7 | (Scaled) | – | – | 37.7 | (Scaled) |
| γ | (–) | Feedback on neutrophil progenitor cells replication to increase/decrease output | 0.149 | (Fixed) | – | – | 0.149 | (Fixed) |
| D _{SLP} | (mL/mg) | Cyclophosphamide linear concentration effect on neutrophil progenitor cells | 1.48 | (13) | – | – | 1.26 | (11) |
| N _{circ,T0} | (N/mL) | Baseline circulating neutrophil count | 2.09 × 10 ⁶ | (1.5) | – | – | 1.69 × 10 ⁶ | (0.7) |
| (Continues) | | | | | | | | |

TABLE 2 (Continued)

| Parameter (units) | Parameter description | Individual models | | Combined in vitro | | Final model | |
|--|-----------------------|--|--------|-------------------|--------|-------------|---------|
| | | Estimate | (RSE%) | Estimate | (RSE%) | Estimate | (RSE%) |
| N_{AMP} | (—) | Surge amplitude/peak describing postinoculation influx of neutrophils into lungs | 52.2 | (17) | — | 44.2 | (24) |
| N_{T0} | (h) | Parameter governing the surge peak time | 50.7 | (3.3) | — | 50.5 | (3.0) |
| N_{SW} | (h) | Parameter governing the surge width | 27.1 | (11) | — | 28.2 | (14) |
| $ERR^a \omega$ | (N/mL) | Additive error term for in vivo neutrophils | 0.151 | (13) | — | 0.161 | (10) |
| Bacterial dynamics and neutrophil-mediated bacterial killing—in vivo | | | | | | | |
| k_{growth} | (h ⁻¹) | Bacterial first-order growth rate constant | 0.489 | (7.7) | — | 0.502 | (18) |
| $k_{N,max}$ | (h ⁻¹) | Neutrophil first-order maximum phagocytosis and digestion rate constant | 1.25 | (29) | — | 0.820 | (33) |
| $k_{N,loss}$ | (h ⁻¹) | Time-related decrease in neutrophil phagocytosis and digestion | 0 | (Fixed) | — | 0 | (Fixed) |
| $k_{M,kill}$ | (h ⁻¹) | First-order rate constant for the additional in vivo phagocytic capacity | 0.279 | (19) | — | 0.287 | (18) |
| $k_{M,loss}$ | (h ⁻¹) | Time-related decrease in the additional in vivo phagocytic capacity | 0.0107 | (48) | — | 0.0111 | (45) |
| $ERR^a \omega$ | (CFU/g) | Additive error term for in vivo CFU | 0.605 | (9.6) | — | 0.600 | (9.4) |

Abbreviation: RSE%, relative standard error in percent.
^aERR refers to the magnitude of residual unexplained variability (on the standard deviation scale).
^bParameters were shared between dig and phag processes.

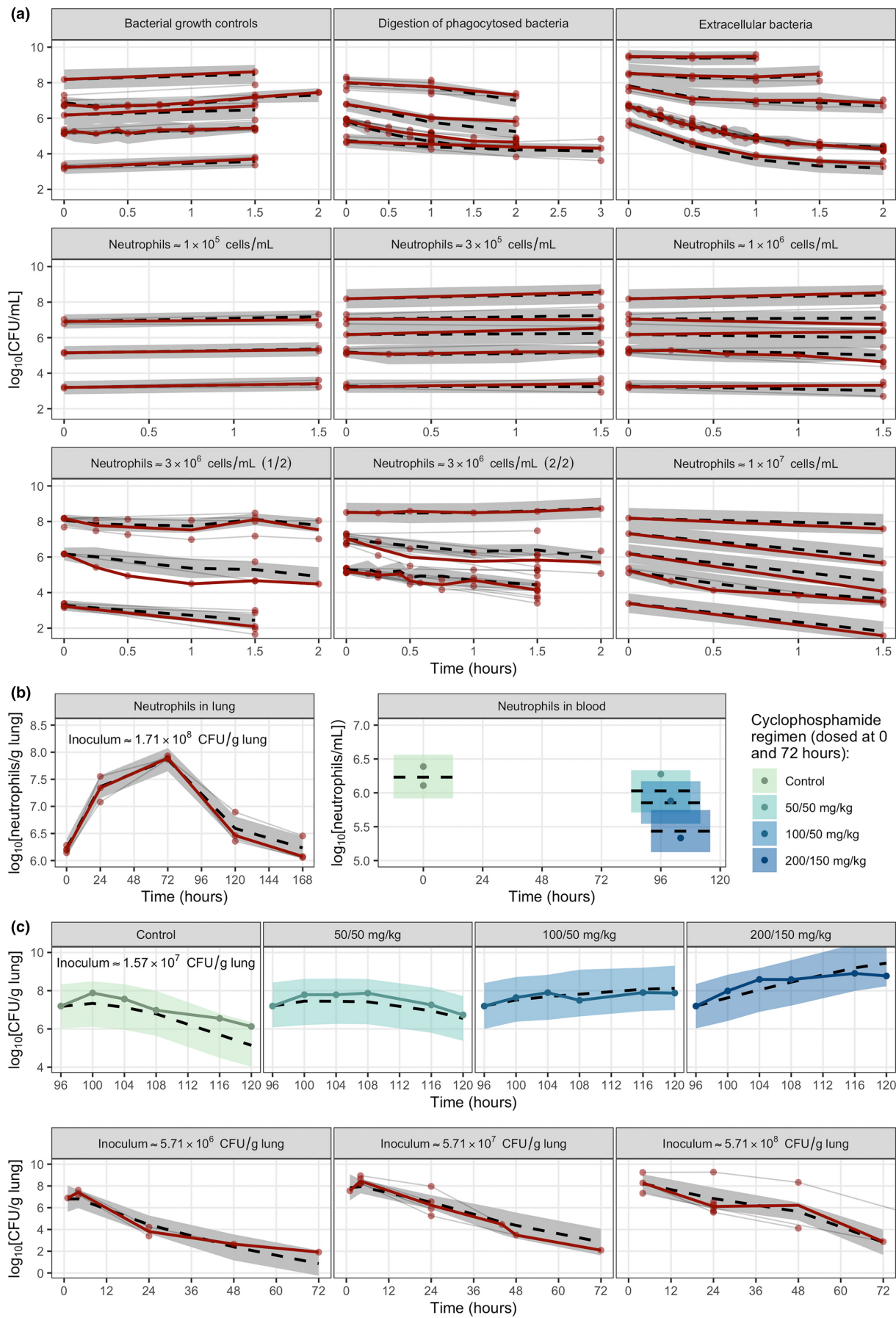


FIGURE 2 Overview of the digitized data used to develop the model and how well simulations from the final model can replicate the digitized time courses. The points represent observations, the solid lines represent the medians of the observations, the dashed lines represent the medians of model simulations, and the shaded areas are 95% confidence intervals for the simulated medians. (a) In vitro studies, covering bacterial growth controls (without addition of neutrophils), digestion of phagocytosed bacteria, extracellular (i.e., nondigested) bacteria, and studies quantifying total bacteria (with approximate neutrophil concentration in the panel headers). (b) In vivo studies measuring neutrophil influx in lungs after administration of bacteria and circulating neutrophils with and without cyclophosphamide treatment (regimen in legend). (c) In vivo studies quantifying the growth of bacteria in the lungs of immune-competent and cyclophosphamide-treated mice. CFU, colony forming unit.

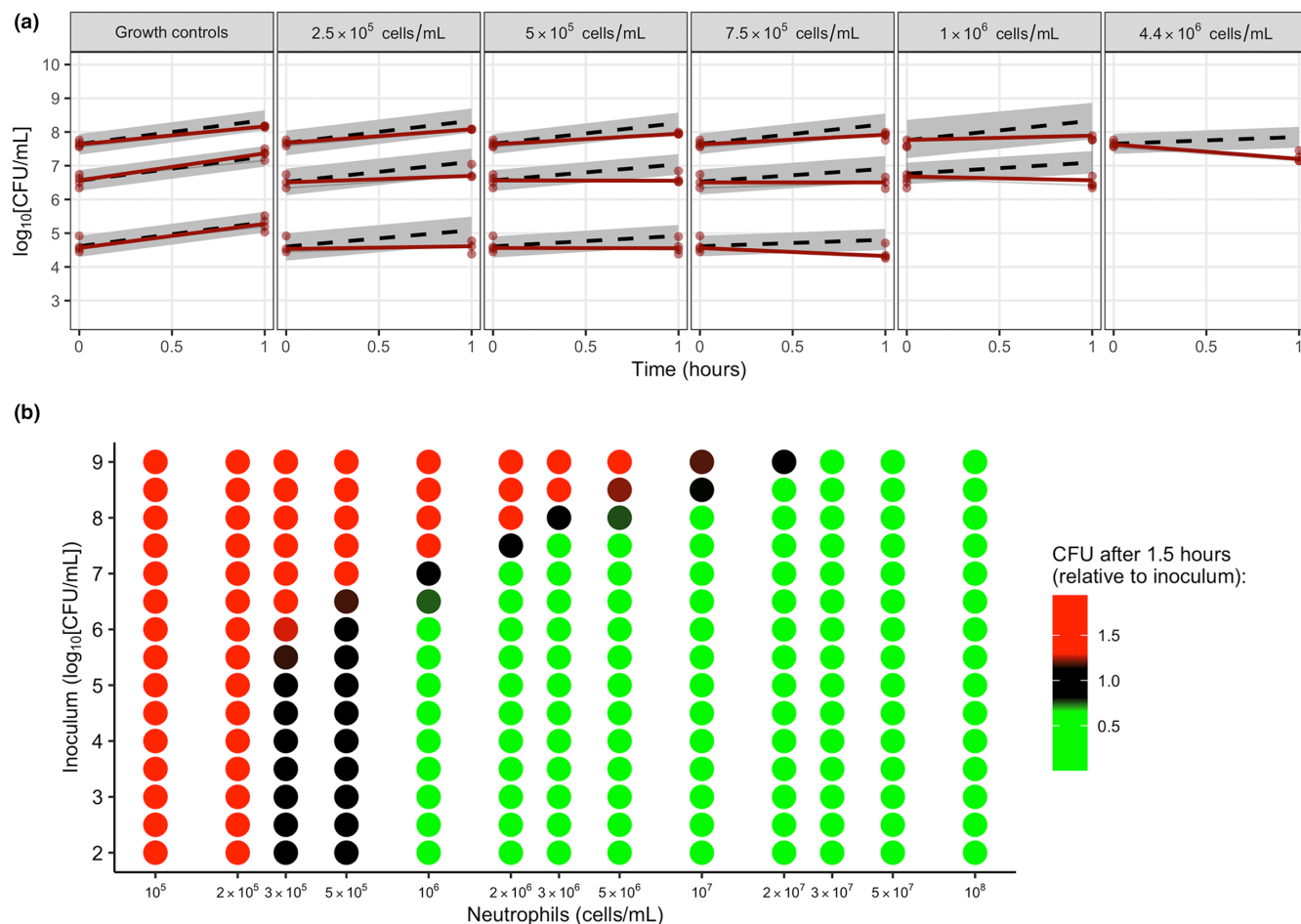


FIGURE 3 (a) Model evaluation on external in vitro data¹⁶ through simulations from the final model. The points represent digitized observations, the solid lines represent the medians of the observations, the dashed lines represent the medians of model simulations, and the shaded areas are 95% confidence intervals for the simulated medians, with the static neutrophil concentration indicated in the header. The lines represent an interpolation between two timepoints (0 and 1 h) and is not a model prediction of the time course. (b) Identification of the same biphasic relation between neutrophil concentration and change in bacterial burden as shown previously.¹⁶ The color represents the colony forming unit [CFU] count relative to the inoculum after 1.5 h, with red indicating an increase, green indicating a decrease, and black indicating minimal-to-no change.

previously developed framework for assessment of bacterial dynamics and antibiotic-induced bacterial killing by linking bacterial concentration to static (in vitro) or dynamic (in vivo) neutrophil concentrations.³⁵ The dynamic neutrophil counts relied on an established model, which has been shown to scale adequately between animals and humans.^{13,34} The model's ability to replicate

the various designs of the underlying data is evident in Figure 2, whereas external evaluation of the in vitro model (Figure 3) was found to slightly underpredict the observed killing. This may reflect a lower maximum system capacity (B_{\max}) in the external data, possibly related to in vitro experimental variability caused by differences in the type of bacteria (clinical isolates vs. reference

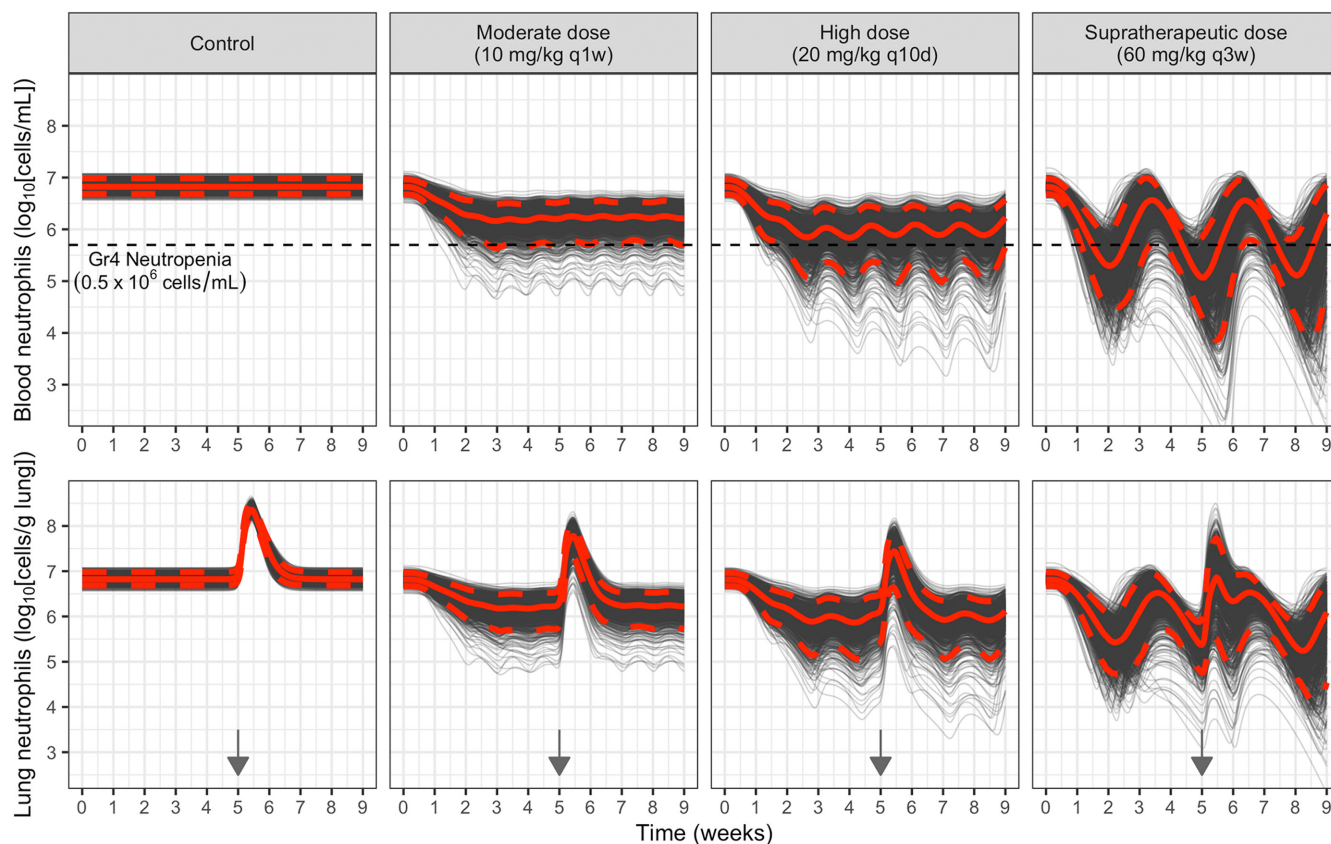


FIGURE 4 Prediction of neutrophil time courses in blood (top) and lung (bottom) for $n = 1000$ individuals (70 kg) treated with cyclophosphamide as indicated in the header (three regimens plus control). Bacteria is deposited in the lungs at 5 weeks (indicated by arrows), which is associated with the surge in lung neutrophil concentration. The red solid lines represent the medians and the dashed red lines the 5th and 95th percentiles of the predictions. The horizontal dashed lines in the top panel indicates the cutoff for Grade 4 (Gr4) neutropenia. q10d, every 10 days; q1w, every week; q3w, every third week.

strains), immune cells (granulocytes vs. neutrophils), or in the experimental set-up. The model did, however, display the same biphasic pattern in CFU change across different bacterial inoculum and neutrophil concentrations, where a neutrophil concentration of 0.5×10^6 cell/mL is enough to deal with bacterial inoculums up to 10^6 CFU/mL, but where progressively higher neutrophil concentrations are required with bacterial inoculums above 10^6 CFU/mL.¹⁶

A potency estimate related to neutrophil-mediated killing of 1.91×10^5 cells/mL has been reported, which is lower than our final estimates of 1.19×10^6 cell/mL for phagocytosis and 6.55×10^6 cell/mL for digestion.²⁷ However, the previous model, which was based on a single study, did not separate phagocytosis and digestion processes or consider the effect of an increasing P/N ratio. Moreover, the study did not use time-varying lung neutrophil concentration (but the circulating count), which may result in a lower estimate. The separation between phagocytosis and digestion was partly informed by intracellular digestion studies^{20,22} and nondigested studies.^{21,23,24} As the estimate of $N_{50,dig}$ was higher than for $N_{50,phag}$ (the fit

was significantly worse with a shared parameter), the digestion process became rate-limiting for removal of bacteria.³⁶ Although the digestion rate would not intuitively depend on the system neutrophil concentration, it may be explained by improved cell-cell interaction and a more even distribution of phagocytosed bacteria across neutrophils at higher neutrophil concentrations.⁴³

The link between the phagocytosis and digestion rates and the P/N ratio may be explained partly through an increased release of antimicrobial peptides, an increased concentration of toxic bacterial products, and an increased stress on the neutrophil cell structure, which compromises the integrity of the neutrophil. An approximate neutrophil capacity of 50 CFU per cell has been reported,⁴⁴ which under the model (P/N_{50}) estimation would result in a 94% reduction of k_{phag} and k_{dig} , irrespective of the neutrophil concentration. A time-dependent decrease of the phagocytosis and digestion rates ($k_{N,loss}$) accounted for progressive in vitro system fatigue, explained by a loss of opsonization and neutrophil deterioration, which may also affect phagosome maturation (important for digestion).^{20,37} The in vitro model development did not account

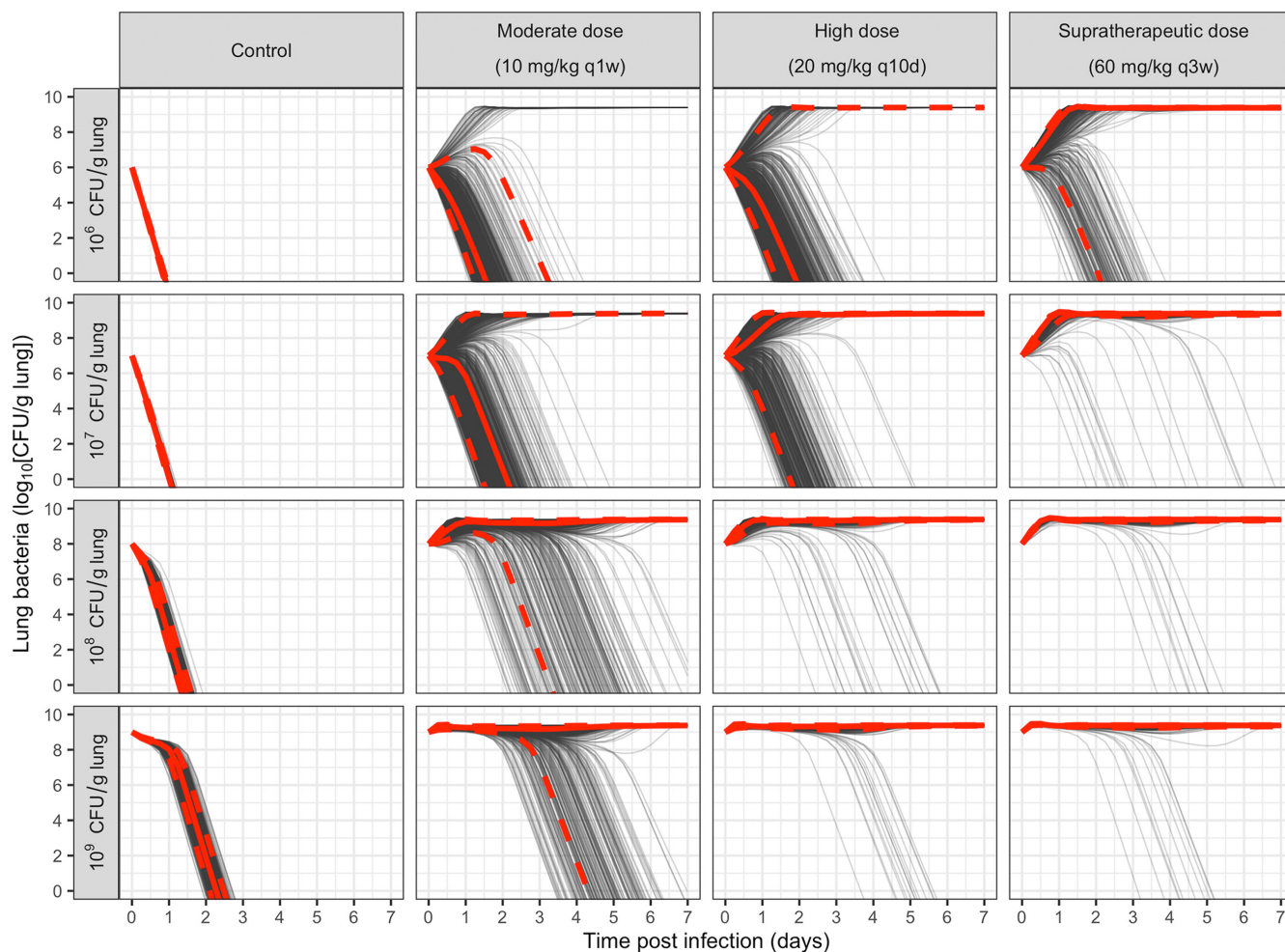


FIGURE 5 Prediction of bacterial time courses in lung for $n=1000$ individuals (70 kg) treated with cyclophosphamide as indicated in the header (three regimens plus control). Neutrophil time courses are as shown in Figure 4, with bacteria deposited in the lungs at 5 weeks. The red solid lines represent the medians and the dashed red lines the 5th and 95th percentiles of the predictions. CFU, colony forming unit; q10d, every 10 days; q1w, every week; q3w, every third week.

for additional bacterial elimination mechanisms, such as extracellular elimination by reactive chemical molecules or extracellular traps.^{11,45}

For the *in vivo* neutrophil dynamics, a postinoculation surge in lung neutrophils was achieved by linking the circulating neutrophil compartment to a compartment representing lungs. Prior to inoculation, the concentration of lung neutrophils (cells/lung) was approximately equal to that in blood (cells/mL), when accounting for lung weight (0.175 g) and/or lung blood volume (0.177 mL).^{30,46} At the peak influx, occurring approximately 2 days postinoculation, the neutrophil lung concentration exceeded 6.31×10^7 cells/g lung, more than 30 \times the circulating concentration. This reaffirms, that the immune response is designed to hit hard and strong, to eradicate pathogens swiftly. However, although the data contained sufficient information to describe neutrophil lung influx, it did not allow for a mechanistic description of the neutrophil source

(i.e., bone-marrow reserves, margined pool) or for inoculum-related differences in influx or increase in circulating counts as infection occurred.⁴⁷ New studies could examine these dynamics further, which would help to determine the extent of the immune system's ability to fight an infection, before neutrophil reserves are exhausted. In the model, the estimate of N_{SW} sustains the neutrophil influx, and all immune-competent mice could eliminate the infection up to the highest inoculum of 5.71×10^8 CFU/g lung (Figure 2). The cyclophosphamide-driven reduction in circulating neutrophils resulted in a lower lung influx, which is sensible as the myelosuppressive therapy is expected to affect neutrophil (and phagocytic) reserves across tissues, with a similar effect on the additional *in vivo* phagocytic capacity (~ 5 -fold reduction). The estimated D_{SLP} of 1.26 mL/mg (neutrophils) was lower than the 2.65 mL/mg (total leukocytes) estimated in rats, even though neutrophils are expected to be more sensitive

to cyclophosphamide than total leukocytes.³⁴ However, given the limited information (no time course) and lack of data on key aspects such as species differences in protein binding and in susceptibility, the re-estimation of D_{SLP} was considered an acceptable option.³⁴

The identified parameter differences in vivo were: (i) a 73% reduced growth rate (k_{growth} of 0.502 h^{-1} , doubling time of 1.38 h), explained by less optimal in vivo growth conditions,⁴⁸ (ii) a 91% decreased maximum neutrophil kill rate ($k_{N,max}$ of 0.820 h^{-1} , $t_{1/2}$ of 0.845 h), which may be explained by a more restricted access of neutrophils to engage with bacteria (not a well-mixed solution, as in vitro), and (iii) removal of the time-driven decrease in activity ($k_{N,loss}$ of 0, as a constant outflow of cells was implemented in the in vivo model). An additional in vivo capacity for phagocytosis was identified, potentially representing lung alveolar macrophages. Although alveolar macrophages are the primary phagocytic cell at baseline conditions they only modestly increase following deposition of bacteria, whereas neutrophils greatly increase in numbers and rapidly make up the majority of phagocytic cells present in lung.^{28,49} The additional phagocytic capacity ($k_{M,kill}$ of 0.287 h^{-1}) resulted in initial bacterial elimination with half-lives of 2.42 h and ~12.1 h in immune-competent and compromised mice, respectively, but reduced over time ($t_{1/2}$ of 62 h) following imitation of the infection. Although the decrease could partly be ascribed to a low influx of new macrophages to the infected tissues (relative to influx of neutrophils), it might also partly reflect the role that macrophages play in phagocytosis of apoptotic and nonapoptotic neutrophils (i.e., phagocytosed instead of bacteria).⁵⁰

Simplifications were made in the description of bacterial dynamics due to the sparse data informing k_{growth} and B_{max} , and the in vitro estimate of k_{growth} covers multiple bacterial species and different studies. The estimate of k_{growth} is comparable to previous estimates of 1.35 h^{-1} for *Streptococcus pyogenes*,³⁵ 1.56 h^{-1} for *S. aureus*, and 1.45 for *E. coli*,¹⁹ whereas the system capacity was fixed to the upper limit of the digitized data. The impact of fixing k_{death} to the value from the original publication (0.179 h^{-1}) was judged to be minor, as any difference in k_{death} would be compensated for in the k_{growth} estimate because those parameters are correlated. Moreover, the data did not support the estimation of k_{RS} , and it was therefore assumed that the bacteria in the resting state would not transfer back to the growing state given the continuous high stress in the environment and the short time frame of the experiments. Similarly, the underlying data did not allow the estimation of differences in neutrophil-mediated killing for different bacterial species. Although this is rational for the

in vitro studies (as a result of well-stirred conditions and proximity between neutrophils and bacteria), the in vivo studies focused on a single species (*A. baumannii*) because of the large between-pathogen variability in stimulation of the innate host response. However, although the model is a general description of neutrophil-mediated bacterial killing, it can readily be expanded with new data and covariate effects such as those describing species differences in growth or kill. Further mouse studies (and modeling efforts) should explore differences in host response and phagocytic capacity toward different bacterial species at different inoculums.

Predictions of human neutrophil and bacterial dynamics (Figures 3–5) indicate that a fixed neutrophil concentration at which all pathogens are successfully eliminated is difficult to derive. Instead, whether a given bacterial inoculum will result in manifestation of eradication depends on the bacterial burden in relation to the neutrophil concentration. In addition, the “critical neutrophil concentration” ($0.3\text{--}0.5 \times 10^6\text{ cell/mL}$) is comparable to Grade 4 neutropenia (Figures 3 and 5), below which the neutrophil number is insufficient to handle even the mildest infections.^{23,24} From Figure 5 (moderate and high dose), it appears that individuals who reach Grade 4 neutropenia (circulating counts) will have difficulties to eradicate the lower burdens of 10^6 and 10^7 CFU/g lung . Indeed, irrespective of patients having neutrophil concentrations above the Grade 4 cutoff, any myelosuppressive drug-induced reduction in neutrophils prevents individuals from dealing with the higher burdens of 10^8 and 10^9 CFU/g lung , whereas untreated subjects are still predicted to eradicate such burdens. However, as these results are extrapolated from mice, clinical data informing the temporal aspects of neutrophil concentration, bacterial burden, and host-response biomarkers (cytokines, chemokines) would help to further elucidate the interindividual variability in host-response mechanisms and phagocytic capacity. The presented model suggests that effective phagocytosis does not only depend on neutrophil concentration, but on the bacterial growth (and natural death) rates and the bacteria-to-neutrophil ratio. As example calculations, the “critical neutrophil concentration” range would result in initial (i.e., phagocytosis at time zero) bacterial $t_{1/2}$'s of 5.73 and 0.724 h in vitro and 5.72 and 3.49 h in vivo, respectively.

In conclusion, we established a model-based description of neutrophil-mediated killing of bacteria through processes of phagocytosis and digestion across in vitro and in vivo studies. The model was used to predict neutrophil-bacterial time courses in patients treated with cyclophosphamide and may be used in the exploration of antibiotic dosing regimens to assess or compare host-response and antibiotic drug effects.

AUTHOR CONTRIBUTIONS

A.T., A.D.P., L.E.F., and E.I.N. wrote the manuscript. A.T., A.D.P., L.E.F., and E.I.N. designed the research. A.T. and A.D.P. performed the research. A.T., A.D.P., L.E.F., and E.I.N. analyzed the data.

FUNDING INFORMATION

The scientific work was supported by The Swedish Cancer Society (CAN 2017/626) and by The Swedish Research Council (VR 2018-03296), and computational resources were funded by The Swedish Research Council (VR 2018-05973).

CONFLICT OF INTEREST STATEMENT

The authors declared no competing interests for this work.

ORCID

Anders Thorsted  <https://orcid.org/0000-0003-1804-2703>

Anh Duc Pham  <https://orcid.org/0000-0002-0279-1761>

Lena E. Friberg  <https://orcid.org/0000-0002-2979-679X>

Elisabet I. Nielsen  <https://orcid.org/0000-0003-0725-214X>

REFERENCES

- Rosales C, Lowell CA, Schnoor M, Uribe-Querol E. Neutrophils: their role in innate and adaptive immunity 2017. *J Immunol Res*. 2017;2017:1-2.
- Summers C, Rankin SM, Condliffe AM, Singh N, Peters AM, Chilvers ER. Neutrophil kinetics in health and disease. *Trends Immunol*. 2010;31:318-324.
- Hidalgo A, Chilvers ER, Summers C, Koenderman L. The neutrophil life cycle. *Trends Immunol*. 2019;40:584-597.
- Neth OW, Bajaj-Elliott M, Turner MW, Klein NJ. Susceptibility to infection in patients with neutropenia: the role of the innate immune system. *Br J Haematol*. 2005;129:713-722.
- Zimmer AJ, Freifeld AG. Optimal management of neutropenic fever in patients with cancer. *J Oncol Pract*. 2019;15:19-24.
- Nesher L, Rolston KVI. The current spectrum of infection in cancer patients with chemotherapy related neutropenia. *Infection*. 2014;42:5-13.
- Maarbjerg SF, Kiefer Lv, Albertsen BK, Schröder H, Wang M. Bloodstream infections in children with cancer: pathogen distribution and antimicrobial susceptibility patterns over a 10-year period. *J Pediatr Hematol Oncol*. 2022;44:e160-e167.
- van Kessel KPM, Bestebroer J, van Strijp JAG. Neutrophil-mediated phagocytosis of *Staphylococcus aureus*. *Front Immunol*. 2014;5:467.
- Dunkelberger JR, Song W-C. Complement and its role in innate and adaptive immune responses. *Cell Res*. 2010;20:34-50.
- Vidarsson G, Dekkers G, Rispen T. IgG subclasses and allotypes: from structure to effector functions. *Front Immunol*. 2014;5:520.
- Segal AW. How neutrophils kill microbes. *Annu Rev Immunol*. 2005;23:197-223.
- Barreto JN, McCullough KB, Ice LL, Smith JA. Antineoplastic agents and the associated myelosuppressive effects. *J Pharm Pract*. 2014;27:440-446.
- Friberg LE, Henningsson A, Maas H, Nguyen L, Karlsson MO. Model of chemotherapy-induced myelosuppression with parameter consistency across drugs. *J Clin Oncol*. 2002;20:4713-4721.
- Maxwell MB, Maher KE. Chemotherapy-induced myelosuppression. *Semin Oncol Nurs*. 1992;8:113-123.
- Abdelraouf K, Nicolau DP. Comparative in vivo efficacies of tedizolid in neutropenic versus immunocompetent murine *Streptococcus pneumoniae* lung infection models. *Antimicrob Agents Chemother*. 2017;61:e01957-16.
- Malka R, Wolach B, Gavrieli R, Shochat E, Rom-Kedar V. Evidence for bistable bacteria-neutrophil interaction and its clinical implications. *J Clin Invest*. 2012;122:3002-3011.
- Nielsen EI, Friberg LE. Pharmacokinetic-pharmacodynamic modeling of antibacterial drugs. *Pharmacol Rev*. 2013;65:1053-1090.
- Bulman ZP, Wicha SG, Nielsen EI, et al. Research priorities towards precision antibiotic therapy to improve patient care. *Lancet Microbe*. 2022;3:e795-e802.
- Leijh PC, van den Barselaar MT, van Zwet TL, Dubbeldeman-Rempt I, van Furth R. Kinetics of phagocytosis of *Staphylococcus aureus* and *Escherichia coli* by human granulocytes. *Immunology*. 1979;37:453-465.
- Leijh PCJ, van den Barselaar MT, Dubbeldeman-Rempt I, van Furth R. Kinetics of intracellular killing of *Staphylococcus aureus* and *Escherichia coli* by human granulocytes. *Eur J Immunol*. 1980;10:750-757.
- Hülshager H, Stangel W, Schmidt J, Potel J. Determination of maximal bactericidal activity in human granulocytes. *Blut*. 1985;50:169-178.
- Pemán J, Cantón E, Hernández MT, Gobernado M. Intraphagocytic killing of gram-positive bacteria by ciprofloxacin. *J Antimicrob Chemother*. 1994;34:965-974.
- Li Y, Karlin A, Loike JD, Silverstein SC. A critical concentration of neutrophils is required for effective bacterial killing in suspension. *Proc Natl Acad Sci U S A*. 2002;99:8289-8294.
- Li Y, Karlin A, Loike JD, Silverstein SC. Determination of the critical concentration of neutrophils required to block bacterial growth in tissues. *J Exp Med*. 2004;200:613-622.
- Knapp S, Wieland CW, Florquin S, et al. Differential roles of CD14 and toll-like receptors 4 and 2 in murine *Acinetobacter pneumoniae*. *Am J Respir Crit Care Med*. 2006;173:122-129.
- van Faassen H, KuoLee R, Harris G, Zhao X, Conlan JW, Chen W. Neutrophils play an important role in host resistance to respiratory infection with *Acinetobacter baumannii* in mice. *Infect Immun*. 2007;75:5597-5608.
- Guo B, Abdelraouf K, Ledesma KR, Chang KT, Nikolaou M, Tam VH. Quantitative impact of neutrophils on bacterial clearance in a murine pneumonia model. *Antimicrob Agents Chemother*. 2011;55:4601-4605.
- Tsuchiya T, Nakao N, Yamamoto S, Hirai Y, Miyamoto K, Tsujibo H. NK1.1(+) cells regulate neutrophil migration in mice with *Acinetobacter baumannii* pneumonia. *Microbiol Immunol*. 2012;56:107-116.
- Casanova-Acebes M, Nicolás-Ávila JA, Li JLY, et al. Neutrophils instruct homeostatic and pathological states in naive tissues. *J Exp Med*. 2018;215:2778-2795.
- Taconic B6 Physiological Data Summary. 2004. Available at: <https://www.taconic.com/phenotypic-data/b6-physiological-data-summary.html>

31. Wickham H, Averick M, Bryan J, et al. Welcome to the tidyverse. *J Open Source Softw.* 2019;4:1686.
32. Wang W, Hallow K, James D. A tutorial on RxODE: simulating differential equation pharmacometric models in R. *CPT Pharmacometrics Syst Pharmacol.* 2016;5:3-10.
33. Keizer R, Karlsson M, Hooker A. Modeling and simulation workbench for NONMEM: tutorial on Pirana, PsN, and Xpose. *CPT Pharmacometrics Syst Pharmacol.* 2013;2:50.
34. Friberg LE, Sandström M, Karlsson MO. Scaling the time-course of myelosuppression from rats to patients with a semi-physiological model. *Invest New Drugs.* 2010;28:744-753.
35. Nielsen EI, Viberg A, Löwdin E, Cars O, Karlsson MO, Sandström M. Semimechanistic pharmacokinetic/pharmacodynamic model for assessment of activity of antibacterial agents from time-kill curve experiments. *Antimicrob Agents Chemother.* 2007;51:128-136.
36. Clawson CC, Repine JE. Quantitation of maximal bactericidal capability in human neutrophils. *J Lab Clin Med.* 1976;88:316-327.
37. Pauwels A-M, Trost M, Beyaert R, Hoffmann E. Patterns, receptors, and signals: regulation of phagosome maturation. *Trends Immunol.* 2017;38:407-422.
38. Jonsson E, Friberg LE, Karlsson MO, et al. Determination of drug effect on tumour cells, host animal toxicity and drug pharmacokinetics in a hollow-fibre model in rats. *Cancer Chemother Pharmacol.* 2000;46:493-500.
39. Movat HZ, Cybulsky MI, Colditz IG, Chan MK, Dinarello CA. Acute inflammation in gram-negative infection: endotoxin, interleukin 1, tumor necrosis factor, and neutrophils. *Fed Proc.* 1987;46:97-104.
40. Bergstrand M, Hooker AC, Wallin JE, Karlsson MO. Prediction-corrected visual predictive checks for diagnosing nonlinear mixed-effects models. *AAPS J.* 2011;13:143-151.
41. FASS Sendoxan. 2022. Available at: <https://libguides.hb.se/c.php?g=522497&p=3572516>
42. Sandström M, Lindman H, Nygren P, Johansson M, Bergh J, Karlsson MO. Population analysis of the pharmacokinetics and the haematological toxicity of the fluorouracil-epirubicin-cyclophosphamide regimen in breast cancer patients. *Cancer Chemother Pharmacol.* 2006;58:143-156.
43. Nguyen GT, Green ER, Meccas J. Neutrophils to the ROScues: mechanisms of NADPH oxidase activation and bacterial resistance. *Front Cell Infect Microbiol.* 2017;7:373.
44. Palmblad J, Engstedt L. Activation of the bactericidal capacity of blood granulocytes. Evaluation of a new method and the effect of levamisole. *Acta Pathol Microbiol Scand C.* 1979;87:357-364.
45. Papayannopoulos V. Neutrophil extracellular traps in immunity and disease. *Nat Rev Immunol.* 2018;18:134-147.
46. Kaul MG, Mummert T, Graeser M, et al. Pulmonary blood volume estimation in mice by magnetic particle imaging and magnetic resonance imaging. *Sci Rep.* 2021;11:4848.
47. Navarini AA, Lang KS, Verschoor A, et al. Innate immune-induced depletion of bone marrow neutrophils aggravates systemic bacterial infections. *Proc Natl Acad Sci U S A.* 2009;106:7107-7112.
48. Dalhoff A. Differences between bacteria grown in vitro and in vivo. *J Antimicrob Chemother.* 1985;15:175-195.
49. Qiu H, KuoLee R, Harris G, van Rooijen N, Patel GB, Chen W. Role of macrophages in early host resistance to respiratory *Acinetobacter baumannii* infection. *PLoS One.* 2012;7:e40019.
50. Silva MT. Macrophage phagocytosis of neutrophils at inflammatory/infectious foci: a cooperative mechanism in the control of infection and infectious inflammation. *J Leukoc Biol.* 2011;89:675-683.

SUPPORTING INFORMATION

Additional supporting information can be found online in the Supporting Information section at the end of this article.

How to cite this article: Thorsted A, Pham AD, Friberg LE, Nielsen EI. Model-based assessment of neutrophil-mediated phagocytosis and digestion of bacteria across in vitro and in vivo studies. *CPT Pharmacometrics Syst Pharmacol.* 2023;12:1972-1987. doi:[10.1002/psp4.13046](https://doi.org/10.1002/psp4.13046)